CO-DIFFUSED BACK-CONTACT BACK-JUNCTION SILICON SOLAR CELLS WITH A NOVEL SCREEN-PRINTED BORON-DOPING PASTE

J.D. Huyeng[1], R. Efinger[1], A. Spribille[1], R. Keding[1], A. Wolf[1], O. Doll[2], F. Clement[1], D. Biro[1]

[1]Fraunhofer Institute for Solar Energy Systems (ISE), Heidenhofstrasse 2, D-79110 Freiburg, Germany
[2]Merck KGaA, Frankfurter Str. 250, D-64293 Darmstadt, Germany

ABSTRACT: Back-contact back-junction silicon solar cells feature high conversion efficiency and have since their introduction been of interest for the photovoltaic community. The interdigitated back-contact design reduces shading losses during illumination but is more complex compared to conventional cell concepts, hampering the industrial integration. This issue has been addressed in research conducted by Fraunhofer ISE and Merck KGaA with the introduction of a screen-printable boron-dopant paste. It allows for cost-reduction in established process routes and enables novel co-diffusion processes with a huge potential. The use of screen-printing avoids high investment costs and makes use of a widely adopted technology. The boron emitter formed during a $POCl_3$:O_2:N_2 co-diffusion process has been characterized by secondary ion mass spectroscopy (SIMS) and quasi-steady state photo conductance (QSSPC). Besides that, a proof-of-principle cell batch has been fabricated based on reference work, with a mean efficiency of 20.9 % over 9 cells (aperture size 4 cm²).
Keywords: Silicon Solar Cell, High-Efficiency, Screen Printing, Interdigitated Back-Contact, Co-diffusion

1 MOTIVATION AND STATE OF THE ART

A concept of interdigitated back-contact (IBC) silicon solar cells was developed by Schwartz and Lammert [1] for concentrator applications. The inherent advantage of the cell architecture is a metal-free front side, which reduces shading losses during illumination. Their prototypes reached an energy conversion efficiency of 17.0 % at 50 suns illumination intensity.

The idea was picked up by other researchers, notably the group of Swanson at Stanford, who shifted the focus to one-sun applications. Since the early 2000's IBC solar cells have been fabricated with active areas exceeding 90 cm². The concept was commercialized under the name Maxeon [2] as a product of the 1985 founded SunPower cooperation. While their early adoption provided them with a lead for many years, contributions to the progression of IBC cells have lately also been made by a number of other companies. Panasonic managed to build todays record holding silicon solar cell with an IBC architecture and the use of silicon heterojunctions. Panasonic's IBC cell features an conversion efficiency of 25.6 % [3] on 143.7 cm². SunPower's latest generation of Maxeon cells utilize passivated contacts, to achieve a mean efficiency of 25.2 % on 153.5 cm², while a number of fabrication details remain confidential [4]. Trina Solar in cooperation with the Australian National University build an IBC solar cell with 24.4 % conversion efficiency based on classical diffusion processes on 4 cm² [5] and recently announced the transformation to 243.36 cm² sized wafers with a resulting efficiency of 23.5 % [6].

The research at Fraunhofer ISE has covered basic research of the cell concept [7, 8], advanced designs [9] and alternative fabrication routes [10] in clean-room environment, as well as industrial integration within the photovoltaic technology evaluation center (PV-TEC [11]). A recent cooperation with Merck has shown the feasibility of inkjet-printed boron-inks [12].

The key issue with industrial integration has often been identified in the increased production costs, as the interdigitated rear-side design is more complex than the industry-dominating Al-BSF design. Following the vast majority of published lab scale fabrication routes, commercialization of IBC solar cells would require an expansion of existing production lines with new equipment, which – besides investment cost – often leads to higher fabrication costs and questionable scaling capabilities. In contrast, the introduction of a process sequence based on established equipment in existing production lines would be an adequate method to bypass these restrictions.

Earlier work by Woehl [13] and Kimmerle [14] explored the use of screen-printed Al-paste, as used in standard processes. Keding [15] investigated the utilization of plasma enhanced chemical vapor deposition (PECVD) for phosphorus- and boron-doped silicate glass coatings (PSG/BSG), as PECVD is already established for the deposition of passivation layers and anti-reflection coatings (ARC). This work will focus once more on the integration of screen-printing (SP) into an industrial feasible process route, by introducing a novel boron-rich paste, to innovate the fabrication of the rear side pattern.

Table I: Results of former work at Fraunhofer PV‑TEC.

		Woehl [13] Al-paste	Keding [16] PECVD
A	(cm²)	16.65	4.0
V_{OC}	(mV)	647	663
J_{SC}	(mA/cm²)	39.4	40.8
FF	(%)	78.4	78.0
η	(%)	20.0	21.1

A key element, being able to further reduce the fabrication costs, is the introduction of a co-diffusion module, as described by Keding and Rothhardt [17]. The necessary prerequisites and the experimental setup to investigate the feasibility of this approach are described in the following.

2 EXPERIMENTAL SETUP

All experiments were performed under semi-industrial conditions in the PV-TEC on Czochralski (Cz) grown large-size (243 cm²) silicon wafers featuring an *n*-type base doping (resistivity 3 Ωcm) if not stated otherwise.

2.1 Co-diffusion

The so-called co-diffusion process reduces the

number of necessary process steps as exemplarily shown in Fig. 1. As dopants are simultaneously driven into the material from different sources, the number of cost-intensive high-temperature steps is minimized (compare left to middle column). In general, this also benefits the wafer quality as less handling and chemical treatment is involved. Additionally, co-gettering has been shown to be advantageous compared to a single diffusion species [18].

	sequential diffusion	co-diffusion (PECVD)	co-diffusion (SP)
1	texture	texture	texture
2a	SiOx – front and rear	PSG/SiOx – rear	
2b	structuring	structuring	
3	diffusion – BBr_3	BSG - rear / B-paste	screen printing – B-paste
3b	removal and cleaning		
4a	SiOx – front and rear		
4b	structuring		
4c	diffusion – $POCl_3$		
4d	removal and cleaning		
5a	SiOx – rear		
5b	diffusion – $POCl_3$	diffusion – $POCl_3$	diffusion – $POCl_3$
6	removal and cleaning	removal and cleaning	removal and cleaning
7	passivation – front and rear	passivation – front and rear	passivation – front and rear
8a	structuring	structuring	
8b	metallization - PVD	metallization - PVD	metallization - SP
8c	structuring	structuring	
9	annealing	annealing	annealing

Figure 1: Schematic process routes.
Orange (dashed) highlighted boxes refer to high-temperature steps. Green (dotted) highlighted boxes include the use of screen-printed boron-paste. The co-diffusion based on PECVD (middle column) offers a vast reduction in process complexity [15]. This paper describes an alteration in process step 3, where boron-paste substitutes BSG. A further reduction is shown in the right column if all PSG layers are substituted by a single $POCl_3$ diffusion process.

To enable this approach, the used sources must not interfere with each other. It has been shown that certain PECVD or APCVD layers can be used with each other (solid diffusion sources [15]) or in combination with a precursor atmosphere [19–21], like gaseous mixtures consisting of phosphorus oxychloride, oxygen, and nitrogen ($POCl_3$:O_2:N_2).

Ultimately, the use of a screen-printed doping source may enable further reduction of process complexity and cost (compare middle and right column), with the metallization possibly also screen-printed. SCost calculations [22] are currently under investigation to evaluate this process in detail, but have already indicated that this should be competitive to both-sides contacted passivated emitter and rear (PERC) concepts.

2.1 Boron-paste investigation

For first investigations concerning the designated novel boron-paste, full area and structured samples were prepared. The application was performed with an industrial screen-printer on large-size wafers. The samples were then treated in an industrial diffusion furnace with a $POCl_3$:O_2:N_2 atmosphere, resulting in the simultaneous formation of highly doped *n*- and *p*-type structures from thermally grown PSG and boron-paste, respectively.

The printing results were analyzed with an optical microscope. The resulting doping structures were visualized with infrared absorption imaging (Sheet-Resistance Imaging [23]), after removal of boron-paste and PSG layers.

The boron doping profile was measured with secondary ion mass spectroscopy (SIMS).

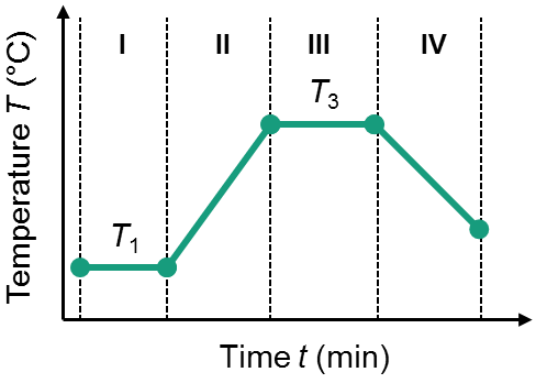

Figure 2: Schematic diffusion process.
A simplified time-temperature diagram is given to illustrate the used diffusion process. The timeframes I-IV refer to different set-temperatures and may in general feature different gas flows to *e.g.* enable the growth of PSG layers from a $POCl_3$:O_2:N_2 atmosphere.

2.2 Passivation quality

To evaluate the effectiveness of surface passivation, symmetrical lifetime samples were fabricated in the same process. Here both sides were covered with screen-printed boron-paste before diffusion. After diffusion, paste removal and cleaning, the samples were coated with atomic layer deposited AlO_x (ALD AlO_x [24]) and PECVD deposited ARC SiN_x on both sides.

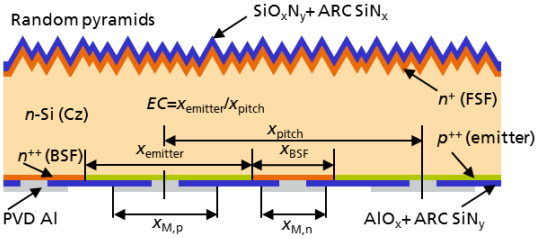

Figure 3: Schematic sample structure.
Arrows and markers give geometrical dimensions used in the text. Colors refer to differently doped or coated layers, as indicated. The front side texture is sketched by random pyramids. All dimensions are not to scale.

The samples were measured with Quasi-steady state photo conductance (QSSPC) on a Sinton WCT-120 setup [25]. The dark saturation current density J_0 was evaluated at high-injection (see details below), according to Kimmerle *et al.* [26].

2.3 Proof-of-principle cell batch

A first batch of (2 x 2) cm² solar cells was fabricated on (15.6 x 15.6) cm² wafers. The front and rear side were covered with PECVD deposited PSG, adjusted for front- and back-surface field (FSF/BSF) formation. The rear side was patterned with a mask-and-etch process involving an inkjet-patterning process module as described by Keding *et al.* [27].

Instead of a PECVD BSG layer a full-area screen-printed boron-paste layer was added on the rear side. Samples were treated in the same diffusion furnace as above.

After diffusion, dopant layer removal and cleaning, the rear side was passivated with a stack consisting of

ALD AlO_x and ARC SiN_x, while the front side was passivated with a $SiriO_xN_y$/ARC SiN_x stack [28]. This is the same setup as used in previous work [15], to emphasize the comparability of boron-paste performance to PECVD BSG.

The rear side's passivation stack and the physical vapor deposited (PVD) Al layer utilized as electrode material was patterned according to the inkjet-pattering process module, as well. Finished solar cells were then tested with an in-house solar simulator and compared with a measurement at the photovoltaic calibration laboratory at Fraunhofer ISE (CalLab) [29].

3 RESULTS

The above described experiments were conducted during fabrication of the proof-of-principle cell batch in order to minimize deviations between test samples and solar cells. If not otherwise stated, measurements were conducted in-house on regularly tested and calibrated equipment.

3.1 Sheet-Resistance Imaging

Sheet resistance imaging as introduced by Isenberg *et al.* allows for spatial analysis of doping structures [30]. The infrared absorption images revealed a distinct contrast between screen-printed regions and prior-to-diffusion bare surface of several hundred counts. The dimensions correlate well with the optically accessible features of the print. The signal was more blurred in a given region compared to a PECVD layer, but measurements were dominated by artifacts in this regard.

3.2 Secondary Ion Mass Spectroscopy

The element sensitive SIMS measurements revealed boron and phosphorus concentrations after $POCl_3$:O_2:N_2 diffusion in a boron-paste covered region after a standard cleaning procedure, as given in Fig. 4. The measurements were performed by CiS GmbH [31].

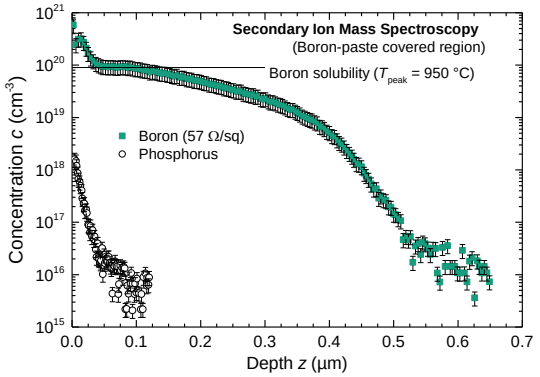

Figure 4: SIMS measurement.
The SIMS signal is calculated for boron and phosphorus species from two measurements on the same sample structure and plotted against the calculated sputter depth. Active boron solubility according to [32]. Details on interpretation are given in the text.

The measured surface concentration of boron exceeds its solubility level in silicon, hinting at remaining precipitates referred to as boron-rich layer [20]. Depth and the resulting sheet resistance of the dopings are comparable to those diffused from BSG, enabling a substitution in this aspect. Boron was never overcompensated by phosphorus, as its concentration is at least two orders of magnitude lower. The used paste can therefore be deemed as a sufficient diffusion barrier during $POCl_3$ diffusion (see Sec. 4).

To avoid the formation of a recombination active boron-rich layer at the surface, the cleaning and the diffusion process have been adjusted in the following.

3.3 Quasi-Steady State Photo conductance

The extracted J_0-values are depicted in Fig. 5. Measurements were performed at different sample positions on multiple wafers. Resulting mean, median and standard deviation values are given by the enclosing box. As a comparison, the mean values of BSG and PSG diffusion are given, as used in the reference process. The BSG and PSG (BSF) regions were passivated alike, while the PSG (FSF) was passivated with $SiriO_xN_y$ and ARC SiN_x, to reproduce the passivation scheme of the solar cell (see Sec 2.3).

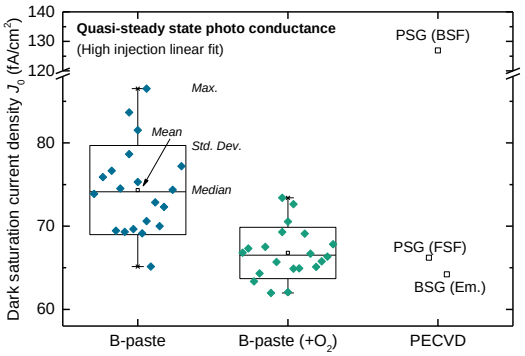

Figure 5: QSSPC measurement results.
The high-injection linear fit results from multiple wafers and different sample positions are given and statistically analyzed. Reference values are given on the right. Details on interpretation are given in the text. (Samples were measured at room temperature, $N_D = 1.3 \times 10^{15}$ cm^{-3}, $n_i = 9.2 \times 10^9$ cm^{-3}, $\Delta n = 1.8\text{-}2.0 \times 10^{16}$ cm^{-3}).

The resulting values are between 65.2 fA/cm² and 86.5 fA/cm² for the standard process. With additional oxidation during cooling (*cf.* Fig. 2, frame IV), an enhancement can be achieved in the mean as well as in the standard deviation, *i.e.* giving a more homogenous process. Its mean value is comparable with the BSG reference, fueling the interchangeability. The given PSG values have been used in numerical simulations (see Sec. 4.1).

3.4 I-V Characteristics

The fabricated cells achieve the same performance level as the reference process [16] within error margins, as could be expected from the emitter characterization. The validity of the average value has been verified by a measurement at Fraunhofer ISE CalLab, perfectly agreeing within the given statistical and systematical errors. These results demonstrate the feasibility of screen-printed boron-rich paste on solar cell level using industrial equipment.

The ideal fill factor FF_0 according to Green [33] could be calculated to 83.9 %, while the pseudo fill factor p*FF* as measured with a Sinton sunsVoc setup was 82.3 %, for the CalLab confirmed cell. The difference p*FF*-*FF*, related to the series resistance, is 3.8 $\%_{abs}$ and is thus greater than the difference FF_0-p*FF* of 1.6 $\%_{abs}$, related to leakage currents.

Table II: IV characteristics of proof-of-principle cell batch (one-sun condition)
Solar cells were fabricated using screen-printed boron-paste and co-diffusion (see Sec. 2.3). The cells were measured with a busbar shading aperture, resulting in an active area of 4 cm² [4].

		Average (9 cells)	FhG ISE CalLab
V_{OC}	(mV)	656 ±3	654 ±2
J_{SC}	(mA/cm²)	41.0 ±0.2	40.0 ±0.8
FF	(%)	77.6 ±0.5	78.9 ±0.5
η	(%)	20.9 ±0.3	20.7 ±0.4

Accordingly, the structure is currently rather limited by series resistance than leakage current, which resembles earlier results from the reference process. The series resistance could be decreased by *e.g.* adjusting the architecture. Leakage currents might be further limited by adjusting the pattern of the passivation stack, manipulating the expansion of the space charge region at silicon's near-surface, or both [19].

4 NEXT STEPS

As shown in the previous paragraph the screen-printed boron-rich paste can be used in the fabrication of IBC solar cells, substituting a cost-intensive PECVD deposition step. Furthermore, the paste has been shown to act as a diffusion barrier during a $POCl_3$:O_2:N_2 involving diffusion process, enabling an even narrower process route (*cf.* Fig. 1), which is the focus of future work.

A simulation of the current preliminary characteristics of the demonstrated cell vehicle shows the influence of the chosen geometry and concludes the investigations at this point.

4.1 Simulation results

Numerical simulations were performed with the freely available QUOKKA 2 [34]. Non-ideal material properties like bulk contaminants were mostly neglected, to focus on the process potential. FSF and BSF regions were modelled according to the reference work, the emitter was adjusted with the measured sheet-resistance and dark saturation current density. Recombination at contacted regions was simulated by EDNA 2 [35] and the profile shown in Fig. 4. The surface recombination velocity at the interface metal/silicon was assumed to be 10^7 cm/s.

A sweep of geometry parameters was performed, keeping the width of the BSF region constant, *i.e.* varying pitch and emitter width and therefore the emitter coverage. Additionally, the metal finger resistance was adjusted according to a geometrical relation.

A relative improvement in conversion efficiency of about 1 $\%_{rel}$ was achieved within simulation, clearly dominated by the fill factor *FF*. A similar improvement could also be achieved by replacing the front surface diffusion by a $POCl_3$:O_2:N_2 process as demonstrated by Tanvir *et al.* [36], according to the simulations.

The development of the simplified process outlined above (see Fig. 1) is expected to yield both: a cheaper fabrication sequence and increased device performance, as understanding of the specific requirements of screen-printed boron-paste grows.

4.2 Challenges for co-diffusion

The challenge in focus of future experiments will be the formation of *p*- and *n*-type doping structures with high resolution and edge sharpness, via co-diffusion. Screen-printed boron-paste will be combined with a $POCl_3$ based diffusion process, in order to fully exploit the huge cost saving potential (see Fig. 1, right column). The involved diffusion sources may not interfere with each other, while also providing sufficient emitter and BSF diffusions to be contacted with screen-printed metallization. Furthermore, the front side diffusion is, in general, different from the rear side BSF, which has in other work been addressed by etch-back experiments [37].

5 SUMMARY

A novel screen-printed boron-doping paste has been shown to enable an industrially feasible process route involving a co-diffusion module in order to fabricate highly-efficient IBC solar cells. In first experiments the fundamental prerequisites of the intended boron-rich paste were investigated and the usability was demonstrated on solar cell level, yielding devices with an average efficiency of 20.9 %. Upcoming experiments will focus on the compatibility of boron-paste and other diffusion sources.

The authors would like to thank S.W. Glunz for fruitful discussion, E. Schäffer for I-V measurements, the whole PV-TEC team at Fraunhofer ISE and the development teams at Merck.

6 REFERENCES

[1] R. J. Schwartz and M. D. Lammert, "Silicon solar cells for high concentration applications," in *1975 International Electron Devices Meeting*, pp. 350–352.

[2] W. P. Mulligan *et al*, "Manufacture of solar cells with 21% efficiency," in *19th EU PVSEC*, 2004, pp. 387–390.

[3] K. Masuko *et al*, "Achievement of more than 25% conversion efficiency with crystalline silicon heterojunction solar cell," *IEEE Journal of Photovoltaics*, vol. 4, no. 6, pp. 1433–1435, 2014.

[4] M. A. Green, K. Emery, Y. Hishikawa, W. Warta, and E. D. Dunlop, "Solar cell efficiency tables (version 47)," *Prog. Photovolt: Res. Appl*, vol. 24, no. 1, pp. 3–11, 2016.

[5] E. Franklin *et al*, "Design, fabrication and characterisation of a 24.4% efficient interdigitated back contact solar cell," *Prog. Photovolt: Res. Appl*, vol. 24, no. 4, pp. 411–427, 2014.

[6] *Trina Solar sets 23.5% IBC cell conversion efficiency record for screen printed process.* [Online] Available: http://www.pv-tech.org/news/trina-solar-sets-23.5-ibc-cell-conversion-efficiency-record-for-screen-prin. Accessed on: May 25 2016.

[7] J. Dicker, J. O. Schumacher, W. Warta, and S. W. Glunz, "Analysis of one-sun monocrystalline rear-contacted silicon solar cells with efficiencies

of 22.1%," *J. Appl. Phys*, vol. 91, no. 7, p. 4335, 2002.

[8] F. Granek, M. Hermle, C. Reichel, O. Schultz-Wittmann, and S. W. Glunz, "High- efficiency back-contact back-junction silicon solar cell research at Fraunhofer ISE," in *23rd EU PVSEC*, 2008, pp. 991–995.

[9] C. Reichel, F. Granek, M. Hermle, and S. W. Glunz, "Back-contacted back-junction n -type silicon solar cells featuring an insulating thin film for decoupling charge carrier collection and metallization geometry," *Prog Photovoltaics*, no. 5, pp. 1063–1076, 2012.

[10] R. Müller *et al*, "Analysis of n-type IBC solar cells with diffused boron emitter locally blocked by implanted phosphorus," *Solar Energy Materials and Solar Cells*, vol. 142, pp. 54–59, 2015.

[11] D. Biro *et al*, "PV-Tec: Retrospection to the three years of operation of a production oriented research platform," in *24th EU PVSEC*, 2009, pp. 1901–1905.

[12] D. Stüwe *et al*, "Inkjet-printed diffusion sources," in *29th EU PVSEC*, 2014, pp. 976–979.

[13] R. Woehl *et al*, "20% Efficient screen-printed and aluminum-alloyed back-contact back-junction cells and interconnection scheme of point-shaped metalized cells," in *37th IEEE Photovoltaic Specialists Conference Seattle: 2011*, 2011, pp. 48–52.

[14] N. Wöhrle, A. Kimmerle, J. Greulich, and A. Wolf, "All-Diffused Back-Contact Back-Junction Solar Cell With Aluminum-Alloyed Emitter—Experiment and Simulation," (English), *IEEE Journal of Photovoltaics*, vol. 6, no. 3, pp. 641–648, http://ieeexplore.ieee.org/iel7/5503869/7456349/07442767.pdf?arnumber=7442767, 2016.

[15] R. Keding *et al*, "Co-diffused back-contact back-junction silicon solar cells without gap regions," *IEEE Journal of Photovoltaics*, vol. 3, no. 4, pp. 1236–1242, 2013.

[16] R. Keding, *Co-diffused Back-Contact Back-Junction Silicon Solar Cells*. Stuttgart: Fraunhofer Verlag, 2015.

[17] R. Keding *et al*, "Silicon doping performed by different diffusion sources aiming co-diffusion," in *27th EU PVSEC*, 2012, pp. 1906–1911.

[18] J. Schön, M. C. Schubert, W. Warta, H. Savin, and A. Haarahiltunen, "Analysis of simultaneous boron and phosphorus diffusion gettering in silicon," *Phys. Status Solidi A*, vol. 207, no. 11, pp. 2589–2592, 2010.

[19] R. Keding *et al*, "$POCl_3$-based co-diffusion process for n-type back-contact back-junction solar cells," in *29th EU PVSEC*, 2014, pp. 676–680.

[20] P. Rothhardt, C. Demberger, A. Wolf, and D. Biro, "Co-diffusion from APCVD BSG and POCl3 for industrial n-type solar cells," *Energy Procedia*, no. 38, pp. 305–311, 2013.

[21] S. Meier *et al*, "Co-Diffusion for P-Type PERT Solar Cells Using APCVD BSG Layers as Boron-Doping Source," in *32nd EUPVSEC 2016*

[22] S. Nold *et al*, "Cost Modeling of Silicon Solar Cell Production Innovation along the PV Value Chain," in *27th EU PVSEC*, 2012, pp. 1084–1090.

[23] J. Isenberg, D. Biro, and W. Warta, "Fast, contactless and spatially resolved measurement of sheet resistance by an infrared method," *Prog Photovoltaics*, vol. 12, no. 7, pp. 539–552, 2004.

[24] A. Richter, J. Benick, and M. Hermle, "Boron Emitter Passivation With Al2O3 and Al2O3 SiNx Stacks Using ALD Al2O3," *IEEE J. Photovoltaics*, vol. 3, no. 1, pp. 236–245, 2013.

[25] A. L. Blum, J. S. Swirhun, R. A. Sinton, and A. Kimmerle, "An updated analysis to the WCT-120 QSSPC measurement system using advanced device physics," in *28th EU PVSEC*, 2013, pp. 1521–1523.

[26] A. Kimmerle, J. Greulich, and A. Wolf, "Carrier-diffusion corrected J0-analysis of charge carrier lifetime measurements for increased consistency," *Solar Energy Materials and Solar Cells*, vol. 142, pp. 116–122, 2015.

[27] R. Keding *et al*, "Diffusion and characterization of doped patterns in silicon from prepatterned boron- and phosphorus-doped silicate glasses," in *26th EU PVSEC*, 2011, pp. 1385–1389.

[28] J. Seiffe *et al*, "Surface passivation of crystalline silicon by plasma-enhanced chemical vapor deposition double layers of silicon-rich silicon oxynitride and silicon nitride," *J. Appl. Phys*, vol. 109, no. 3, p. 34105, 2011.

[29] *CalLab PV Cells / CalLab PV Modules — Fraunhofer ISE*. [Online] Available: https://www.ise.fraunhofer.de/en/service-units/callab-pv-cells-callab-pv-modules. Accessed on: Jun. 06 2016.

[30] J. Isenberg, M. C. Schubert, D. Biro, A. Froitzheim, and W. Warta, "Sheet resistance imaging (SRI) - A contactless and spatially resolved method for the determination of doping inhomogeneities," in *20th EU PVSEC*, 2005, pp. 674–677.

[31] CiS Forschungsinstitut für Mikrosensorik und Photovoltaik GmbH, *CiS :: Willkommen bei CiS*. [Online] Available: http://www.cismst.org/. Accessed on: May 25 2016.

[32] D. Nobili, "Solubility of B in Si," *Properties of Silicon*, p. 384, 1987.

[33] M. A. Green, "Solar cell fill factors: General graph and empirical expressions," *Solid State Electron*, vol. 24, no. 8, pp. 788–789, 1981.

[34] A. Fell, "A free and fast three-dimensional/two-dimensional solar cell simulator featuring conductive boundary and quasi-neutrality approximations," *IEEE Trans. Electron Devices*, vol. 60, no. 2, pp. 733–738, 2013.

[35] K. R. McIntosh *et al*, "An Examination of Three Common Assumptions Used to Simulate Recombination in Heavily Doped Silicon," in *28th EU PVSEC*, 2013, pp. 1672–1679.

[36] N. B. Tanvir *et al*, "Codiffusion Sources and Barriers for the Assembly of Back-Contact Back-Junction Solar Cells," *IEEE J. Photovoltaics*, vol. 5, no. 6, pp. 1813–1820, 2015.

[37] A. Kimmerle, "Diffused Surfaces For Crystalline Silicon Solar Cells: Process Development, Characterization, and Modeling," Dissertation, IMTEK, Albert-Ludwigs-University, Freiburg, 2015.